Physica A 606 (2022) 128129

Contents lists available at ScienceDirect

Physica A

journal homepage: www.elsevier.com/locate/physa

# Investigating traffic safety reckoning hyperbolic driving following behavior using trajectory data

Narayana Raju [a,*], Shriniwas Arkatkar [b], Constantinos Antoniou [c]

[a] Delft University of Technology (TU Delft), The Netherlands
[b] Sardar Vallabhbhai National Institute of Technology, Surat, India
[c] Technical University of Munich (TUM), Germany

ARTICLE INFO

*Article history:*
Received 16 February 2022
Received in revised form 27 July 2022
Available online 27 August 2022

*Keywords:*
Instantaneous heeding time
Rear-end collisions
Hysteresis
Hyperbolic vehicle-following

ABSTRACT

Using vehicle trajectory datasets developed over a study section for three traffic flow levels, a rectangular hyperbolic relation between time-to-collision and relative speeds in vehicle-following behavior were observed. A new methodology for estimating the probable rear-end collisions in the given traffic stream is developed based on this relation. The vehicle-following behavior is examined in terms of the hysteresis phenomenon concerning the distance gap (DG) and relative speed (RS). Further, based on the follower's attention towards the leader vehicle, a novel surrogate safety measure, called Instantaneous Heeding Time (IHT), was conceptualized. This measure represents the time gap available based on the positions of the leader and follower vehicles. After exploring vehicle-following behavior, IHT, DG, and RS were used to estimate the rear-end collision probability. The applicability of the proposed methodology is tested using different thresholds (IHT, DG, and RS) and applied to the study section at the three traffic flow levels.



## 1. Introduction

Traffic safety is one of the major issues in the ever-growing transportation. To assess the safety and limit the damage before the occurrence of crashes, researchers focused on proactive safety methods. This led to the idea of surrogate safety measures (SSMs). In this direction, research attempts are observed from the early 1970s and progressed over time. In this direction, Hayward [1] formulated the idea of Time-To-Collision (TTC). On similar lines, numerous SSMs are evolved/developed over time, which includes Time integrated TTC (TIT) [2], (3) Time exposed TTC (TET) [3], (4) Deceleration rate to avoid collision (DRAC) [4], and (5) Collision potential index (CPI) [5] etc.

Further to understand the severity, risk and label the collision events, researchers integrated the early developed SSMs with other behavior characteristics. This led to the development of Traffic Conflict Techniques (TCT's). In this direction, authorities from various developed nations framed their TCTs [6]. Based on these measures, numerous studies have been reported worldwide such as TTC in collision avoidances [7], TTC at automation scenarios [8], vehicle–pedestrian interactions [9], and rear-end collisions identification based on TTC[10]. Currently, SSMs found a place across various levels of traffic safety studies, which includes Traffic microsimulation [11–13], empirical analysis [14–16], driving simulator experiments [17–19], virtual reality experiments [20–22] etc.

* Corresponding author.
*E-mail addresses:* s.s.n.raju@tudelft.nl (N. Raju), sarkatkar@gmail.com (S. Arkatkar), c.antoniou@tum.de (C. Antoniou).

https://doi.org/10.1016/j.physa.2022.128129

**Table 1**
Acronyms used in the present manuscript.

| Acronym | Description |
|---|---|
| PCU | Passenger Car Units |
| MThW | motorized three-wheelers |
| MTW | motorized two-wheelers |
| LCV | light commercial vehicles |
| V/C | Volume to capacity |
| DG | distance gap (m) |
| RS | relative speed (m/s) |
| IHT | Instantaneous Heeding Time (s) |
| TTC | Time-To-Collision (s) |
| FV | follower speed (m/s) |
| LV | leader speed (m/s) |
| $X_L$ | longitudinal position of the leader vehicle (m) |
| $X_F$ | longitudinal position of the follower vehicle (m) |
| $l$ | length of the leader vehicle (m) |

Further, it was inferred that, in most instants, the time gap between vehicles is evaluated and related to safety. With the deceleration concept, braking/deceleration is modeled as a function of time prior at the time of the collision. The following driver paid attention to the leader vehicle (or only the leader). However, there is no general rule in real field conditions that a follower driver, just about to have a rear-end collision with its leader, decelerates at a high rate.

Based on driving behavior studies [23–26], it can be understood that quantifying driving behavior along with other parameters such as time gap between two consecutive vehicles can be a significant potential component in understanding the safety. All these studies are conducted in developed countries, which is mainly possible due to collision data availability at the micro-level. On the contrary, developing reliable and accurate collision data is relatively tricky in emerging countries. In these countries, generally, there is a presence of multi-class vehicles ranging from small-size vehicles such as motorized two-wheelers to large-size vehicles such as buses and trucks. This traffic mix makes traffic stream highly heterogeneous due to the varying static and dynamic characteristics of the vehicles.

In the case of mixed traffic conditions prevailing in countries like India, very few studies were attempted to capture driving behavior as a function of vehicle and maneuver types across different roadway and traffic conditions [27–30]. From these studies, it can be noted that the numerous vehicle categories and ensuing weak lane-discipline result in complex interactions among the vehicles. Even automated data collection techniques have primarily failed in capturing traffic movements accurately. This study was initiated with the intent of studying driving behavior under mixed traffic conditions prevailing in India. Initially, based on an illustrated video survey from the study section, trajectory data were developed as the first step with the help of a semi-automated tool. Further, based on the investigation of vehicle-following behavior among different vehicle pairs, a new surrogate safety measure, named Instantaneous Heeding Time (IHT), was suggested in evaluating rear-end collisions.

## 2. Research methodology

The proposed methodology involves five phases (Fig. 1): (1) data collection and preparation, (2) hysteresis and hyperbolic analysis, (3) developing attention measure for the follower driver, (4) probabilistic modeling of rear-end collision, and (5) safety analysis. In Phase 1, the study section is identified, followed by video graphic surveys and trajectory data development. In Phase 2, the vehicle-following behavior of the vehicles is examined using TTC and relative speed. In Phase 3, drivers' attention in the following conditions is quantified concerning IHT. In the fourth phase, attention of drivers in following conditions are quantified with respect to Instant Heeding Time (IHT), relative distances and follower vehicle speed. Finally, in Phase 5, safety analysis is performed, and guidance related to predicting rear-end collisions under varying mixed traffic conditions is established. The next sections present the data collection process and hysteresis and hyperbolic analysis. The following sections present the safety analysis using the developed methodology. Practical implementations are then presented, followed by summary and conclusions. Further to facilitate the readers, the list of acronyms are used in the study are presented in Table 1.

## 3. Data collection

A midblock on a multilane high-speed road in Mumbai, India, is selected to examine the driving behavior in the present work. The roadway facility is a ten-lane carriageway with a total width of 17.5 m per direction and 120-m trap length. The roadway facility is selected in such a way that it includes varying roadway and traffic characteristics. Based on this, a 12-hour video graphic survey was conducted to record traffic characteristics in terms of video data of running traffic flow. Macroscopic traffic flow characteristics were evaluated in terms of Passenger Car Units (PCU) factors with a capacity of around 11,800 PCU/h [31]. Vehicular trajectory data is developed to understand the microscopic traffic flow interactions among vehicles. To accomplish this, a semi-automated image processing tool is used in extracting the trajectory data. In

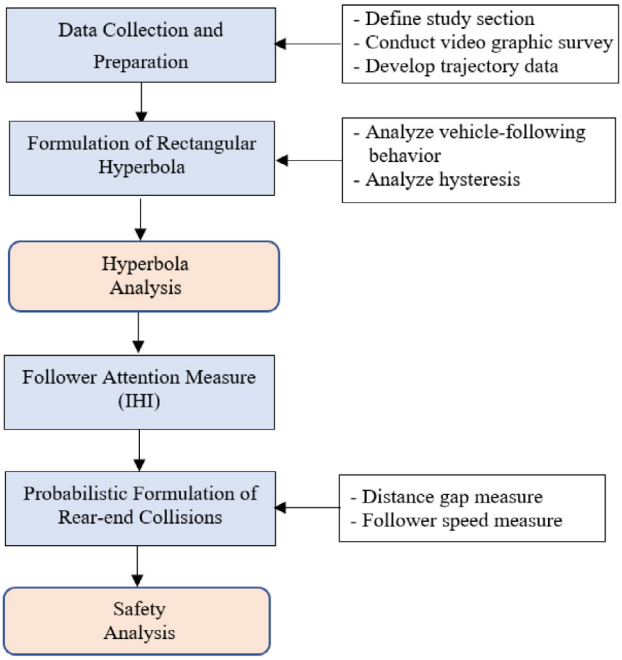


**Fig. 1.** Methodology on Investigating Traffic Safety Reckoning Hyperbolic Driving Following Behavior.


**Fig. 2.** Snapshots from the study sections for different traffic flow levels: (a) free flow, (b) near-capacity flow, and (c) congested flow.

line with the literature, to limit the noise in trajectory data, smoothening techniques were applied [32,33]. To understand the variation in driving behavior, trajectory data were developed for three traffic flow levels: free flow, near-capacity flow, and congested flow. The details of the data are shown in Table 2. Snapshots of the study sections and the developed time–space plots of vehicles observed during real-field conditions on the western expressway are shown in Figs. 2 and 3. The present study involves six dominant vehicle categories: motorized three-wheelers (MThW), motorized two-wheelers (MTW), buses, cars, trucks, and light commercial vehicles (LCV).

## 4. Hysteresis and hyperbolic analysis

### *4.1. Hysteresis analysis*

To understand the safety implications in mixed traffic streams, vehicle-following behavior was examined. The core logic of the car-following model by Wiedemann [34] which quantifies the following-behavior based on distance gap (DG) and relative speed (RS), was considered. Relative speed is defined as follower speed (FV) minus leader speed (LV). Based on this, with the help of the developed trajectory data, the vehicle-following behavior is examined. Using a MATLAB code, vehicle category involving DG vs. RS is plotted among the subsequent vehicles with lateral overlap, and the leader–follower pairs are identified.

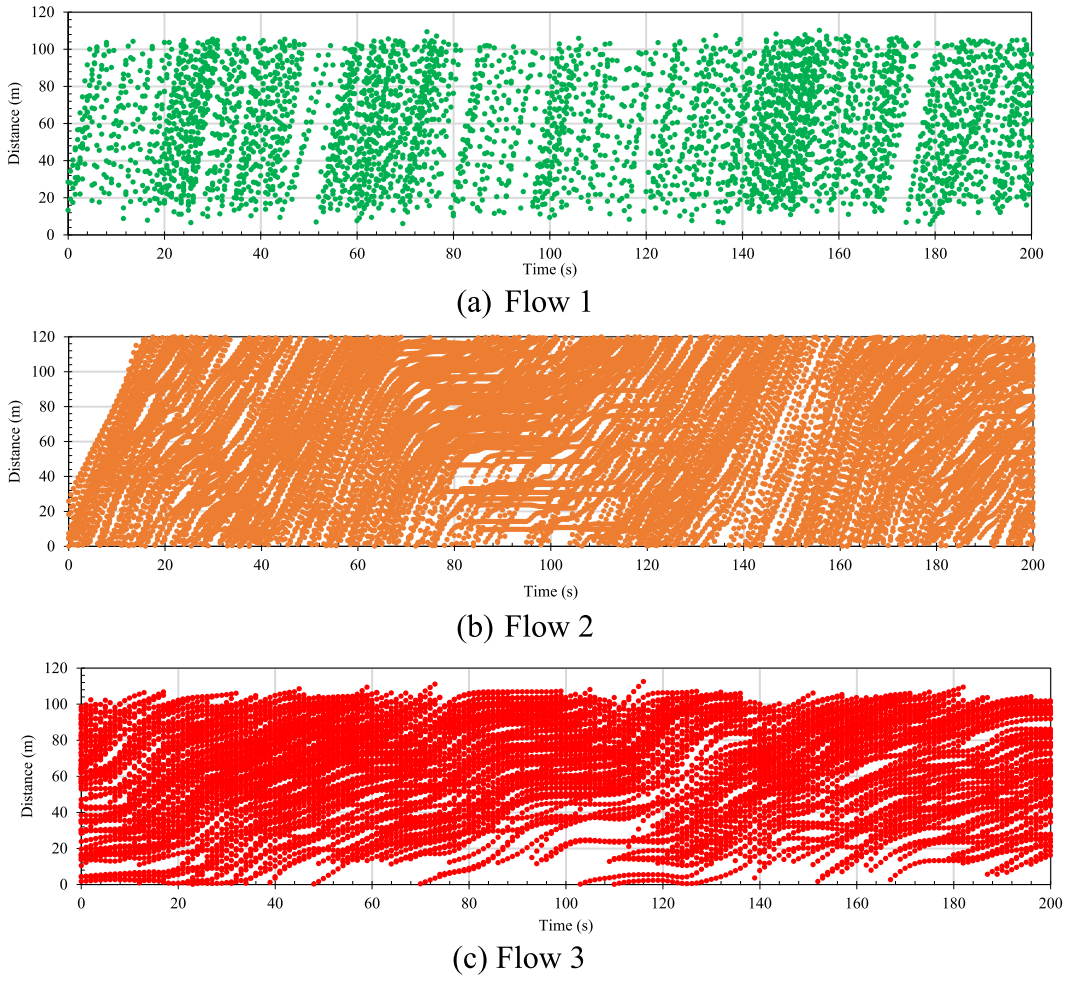


**Fig. 3.** Time–space plots of vehicles for different traffic flow levels.

**Table 2**
Details of trajectory datasets over the study section.

| Trap length (m) | Road width (m) | Traffic flow level | Traffic Compo.[a] | Traffic flow parameters | | V/C | No. of vehicles tracked | Duration[b] (min) |
|---|---|---|---|---|---|---|---|---|
| | | | | Avg. Speed (km/h) | Avg. Flow (pcu/h) | | | |
| 120 | 17.5 | Free | 15/35/5/40/2/3 | 65 | 4800 | 0.4 | 1080 | 15 |
| | | Near-capacity | 20/29/2/45/1/3 | 42 | 10120 | 0.85 | 1715 | 15 |
| | | Congested | 17/25/5/45/3/4 | 20 | 3500 | < 1 | 660 | 10 |

[a]Traffic composition: Motorized three wheelers /Motorized two-wheelers/Bus/Car/Truck/LCV.
[b]Duration of trajectory data.

Further, based on the followers' vehicle categories, the plots are aggregated for different flow levels, as shown in Fig. 4. From the following behavior analysis, the hysteresis shape is marginally noted in Flow 1 (free flow). On the other hand, beyond free flow, the definite hysteresis shape is observed among the pairs, whereas for Flow 3, the hysteresis shape among the vehicles tends to be slender with reductions in RS and DG. The results show a wide variation in driving behavior, which can be observed in the traffic stream as traffic flow level varies. Also, it may be noticed that there is a wide variation in vehicle-following behavior when the type of the following vehicle varies from smaller to heavy vehicles. For example, DG = 0 to 30 m, 0 to 20 m, and 0 to 10 m, the difference in RS for smaller vehicles (MTW, MThW, and MTW as followers) are observed to be in the range of −10 m/s to 10 m/s. In contrast, for heavy vehicles (Bus, Trucks, and LCV as following vehicles), this range is −5 m/s to 5 m/s. The larger scale of RS difference indicates aggressive behavior. This behavior is consistent with the real field recorded observation. For smaller vehicles, such as MTW and MThW, drivers

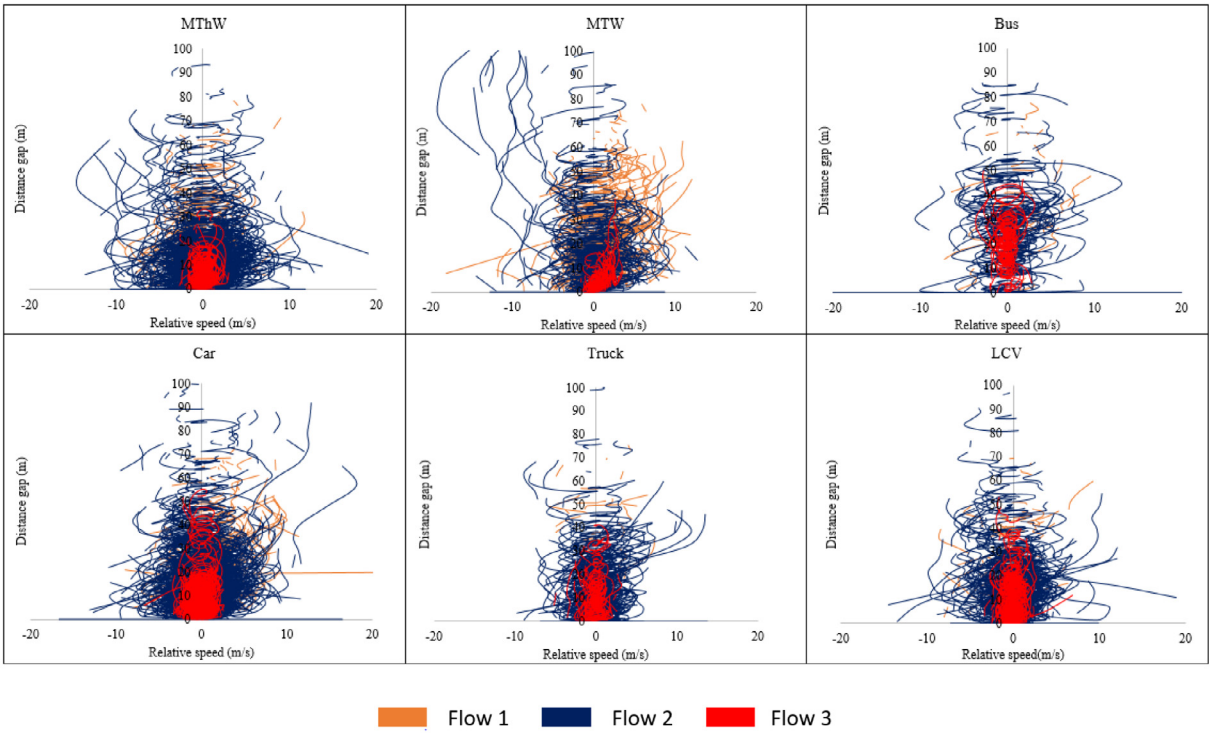


**Fig. 4.** Distance gap vs relative speed for different types of vehicles.

tend to choose maneuvers based on the availability of road space, hence substantially deteriorating safety in the traffic stream. This study has focused on developing surrogate safety measure, which can incorporate the effect of these smaller vehicles' aggressiveness in accurately predicting rear-end collisions.

### *4.2. Hyperbolic analysis*

One possible way to determine the probability of rear-end collision is to develop measures such as TTC. In the literature, numerous studies reported TTC as a measure for quantifying safety by predicting the number and severity of collisions. TTC [1,35] is also computed using trajectory data derived from the extracted leader–follower pairs in the present research work. In classical form, TTC is calculated when follower speed exceeds the leader speed. As a result, the TTC magnitude is always positive. However, in the present work, to reveal the TTC phenomenon profoundly and its play in following behavior between the vehicles, the negative part of the TTC is presented.

Further, the calculated TTC values are checked for its correlation with RS at a given instant among the leader–follower couples. The plots were drawn considering different vehicle types, as the following vehicles are shown in Fig. 5. Interestingly, those plots tend to depict a distinct rectangular hyperbolic pattern for all datasets plotted of different vehicle categories. To the best of the author's knowledge, no earlier study has reported a hyperbolic model in driving behavior under mixed traffic conditions. These patterns are also likely to be produced for traffic situations prevailing in developed countries where lane-disciplined driving practices are followed. Further, with an increase in traffic flow level, the shape tends to vary, as Flows 1 and 2 (Fig. 5) show, where a clear hyperbola is visualized. For Flow 3, the data points tend to shift close towards the TTC axis (y-axis)

To formulate the observed hyperbolic phenomenon, the traditional hyperbola was examined. In general, the hyperbola is given by

$$\frac{x^2}{a^2} - \frac{y^2}{b^2} = 1 \tag{1}$$

with asymptotes, $y = \pm\frac{b}{a}x$, where $x$ and $y$ are intercepts and a and b are constants.

In the case of rectangular hyperbola with eccentricity equal to $\sqrt{2}$, the constant terms will be equal (a = b), and Eq. (1) is written as

$$\frac{x^2}{a^2} - \frac{y^2}{a^2} = 1 \tag{2}$$

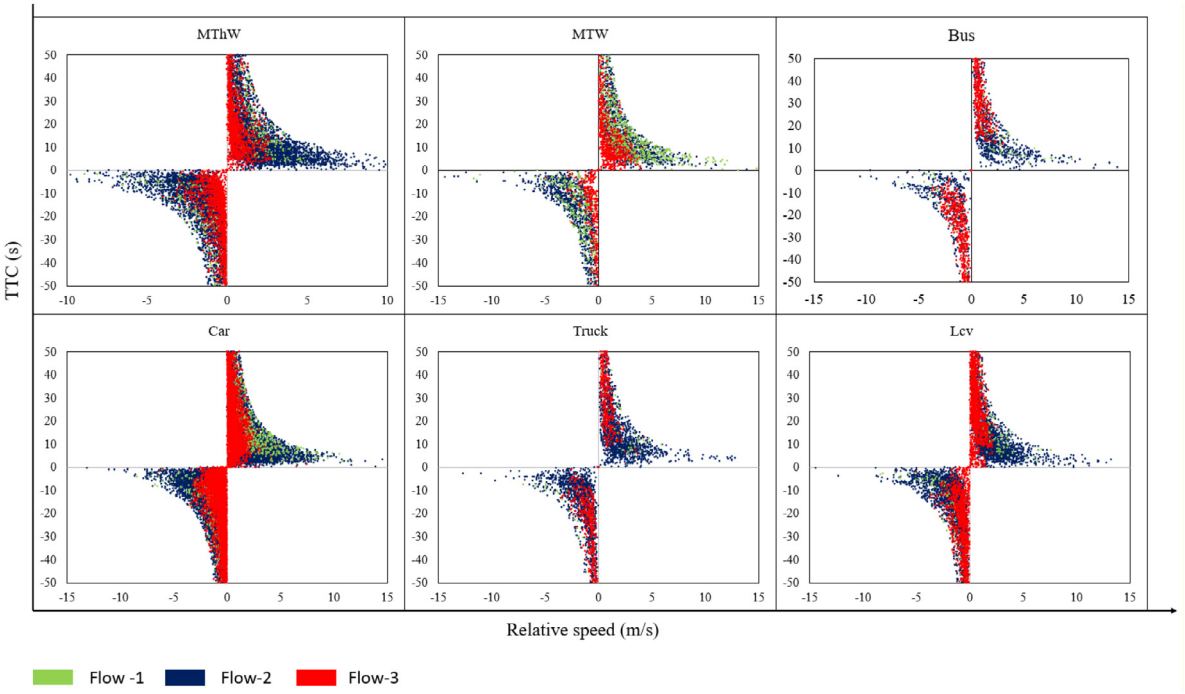


**Fig. 5.** Rectangular hyperbolic formulation in between TTC vs RS.

$$x^2 - y^2 = a^2 \tag{3}$$

In comparison with the traditional hyperbola, the axis of the rectangular hyperbola is inclined at $45^0$ to the traditional Cartesian axis. Therefore, the intercepts in the rectangular hyperbola case are *RS* on the *x*-axis and TTC on the *y*-axis. Hence,

$$\begin{pmatrix} x \\ y \end{pmatrix} = \begin{pmatrix} \cos\theta & \sin\theta \\ -\sin\theta & \cos\theta \end{pmatrix} \begin{pmatrix} RS \\ TTC \end{pmatrix} \tag{4}$$

$$\begin{pmatrix} x \\ y \end{pmatrix} = \begin{pmatrix} \frac{1}{\sqrt{2}} & \frac{1}{\sqrt{2}} \\ -\frac{1}{\sqrt{2}} & \frac{1}{\sqrt{2}} \end{pmatrix} \begin{pmatrix} RS \\ TTC \end{pmatrix} \tag{5}$$

In another form, the coordinate conversion is given as

$$x = \frac{RS}{\sqrt{2}} + \frac{TTC}{\sqrt{2}} \tag{6}$$

$$y = -\frac{RS}{\sqrt{2}} + \frac{TTC}{\sqrt{2}} \tag{7}$$

Substituting for *x* and *y* from Eqs. (6) and (7) into Eq. (3), then the traditional hyperbola is given by

$$RS * TTC = \frac{a^2}{2} \tag{8}$$

$$RS * TTC = Constant \tag{9}$$

where Constant $= a^2/2\ (> 0)$.

Further, to interpret the rectangular hyperbolic pattern in a detailed manner, the TTC vs RS data points are segregated based on DG bands taking intervals of 10 m and plots are plotted as shown in Fig. 6. It was observed that based on the distance gap bands, individual hyperbola patterns are visualized. As discussed in the above sections, with variation in flow levels, eccentricity in plots is observed. For example, in the case of Flow-1, under free-flow conditions, the data points are sparse with appropriate shapes. In the case of Flow-2, near capacity level flow, further, clear rectangular hyperbola space is observed with reasonably good density points. On the other hand, in the case of Flow-3, involving stop-and-go conditions, no data points are observed at the relative spacing of more than 45 m and data is observed to be more shifted to the TTC axis (Y-axis) having less RS, which is also an indication of constraint in movements. Similarly, with the increase

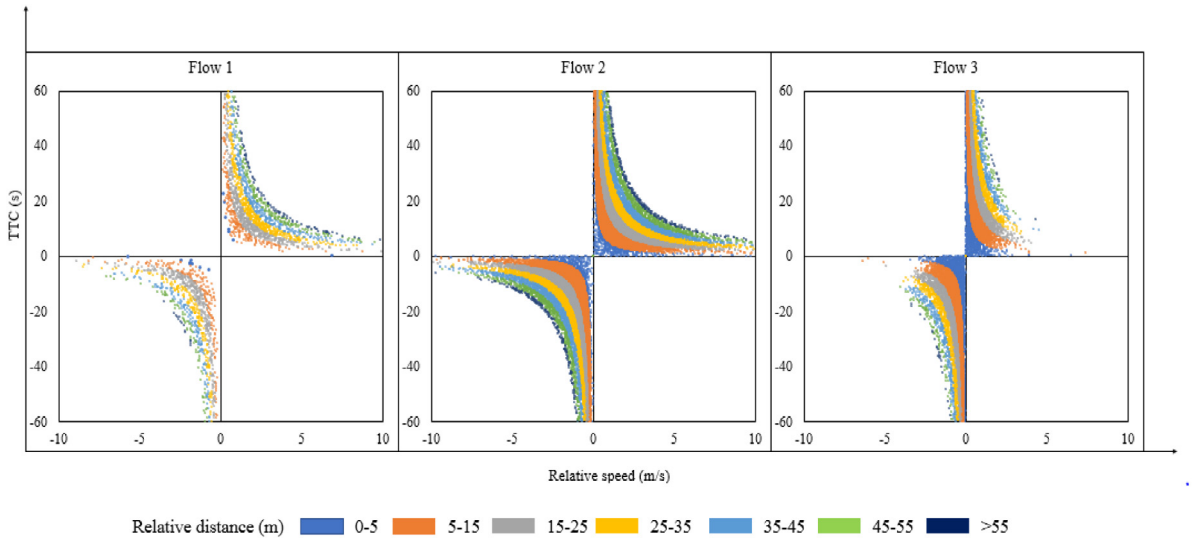


**Fig. 6.** Hyperbolic relation between RS and TTC for different DG bands.

**Table 3**
Analytics of rectangular hyperbolic pattern.

| Distance gap band (m) | Vertex (m/s, s) | | Foci (m/s, s) | | Length of latus rectum (m) |
|---|---|---|---|---|---|
| 0–5 | (2.5, 2.5) | (−2.5, −2.5) | (3.53,3.53) | (−3.53, −3.53) | 7.07 |
| 5–15 | (10, 10) | (−10, −10) | (14.14, 14.14) | (−14.14, −14.14) | 28.28 |
| 15–25 | (20, 20) | (−20, −20) | (28.28, 28.28) | (−28.28, −28.28) | 56.56 |
| 25–35 | (30, 30) | (−30, −30) | (42.42, 42.42) | (−42.42, −42.42) | 84.85 |
| 35–45 | (40, 40) | (−40, −40) | (56.56, 56.56) | (−56.56, −56.56) | 113.13 |
| 45–55 | (50, 50) | (−50, −50) | (70.71, 70.71) | (−70.71, −70.71) | 141.42 |
| >55 | (57, 57) | (−57, −57) | (80.61, 80.61) | (−80.61, −80.61) | 161.22 |

of DG, the focus of those hyperbola patterns is shifted away from the origin. Hence, it was decided that in this research work, rectangular hyperbola metrics, such as vertices, foci and length of latus rectum, can be evaluated based on the distance gap bands, the results for which are as presented in Table 3. It is evident that with an increase in distance gaps, all those metrics tend to increase and hence strongly advocate the constant terms in Eq. (9), as distance gaps, particularly under the vehicle-following conditions, at a given flow level.

For a given flow level, with the observed following behavior showing hysteresis for different vehicle types, TTC was computed as the line's slope, which tends to form a kind of cone shape. Further, the RS cuts them upright as an edge slicing the cone, creating the traditional rectangular hyperbola concept of a regular plane cutting the cone. As a result, the square hyperbolic formulation was observed in the vehicle-following conditions. Further, in the present case of the following behavior scenario at a given flow level, *DG* has naturally taken the form of a constant. Then, based on Eq. (9),

$$TTC = \frac{DG}{RS} \ (where\, DG > 0) \tag{10}$$

which is the traditional equation for computing *TTC*.

*Opening–Closing Zone Interpretation*

After a careful examination of the hysteresis and rectangular hyperbola plots, it was observed that in the closing process, when FV is higher than LV, both RS and TTC have positive values. On the other hand, during the opening process, when FV is less than LS, both RS and TTC have negative values. Further, from the hysteresis plots, it can be anticipated that the first quadrant replicates the closing process of follower–leader pairs, and the fourth quadrant represents the opening process of follower–leader pairs, as shown in Fig. 7. In hyperbola plots, the closing and opening processes are observed in the first and third quadrants, respectively, as shown in Fig. 8. This interpretation can help understand driver behavior concerning longitudinal movements, mainly when the vehicle-following phenomenon is observed. Besides, the analysis would clarify the procedure for predicting rear-end collisions using probability concepts and would be useful in understanding a newly developed surrogate safety measure, Instantaneous Heeding Time (IHT), as discussed later.

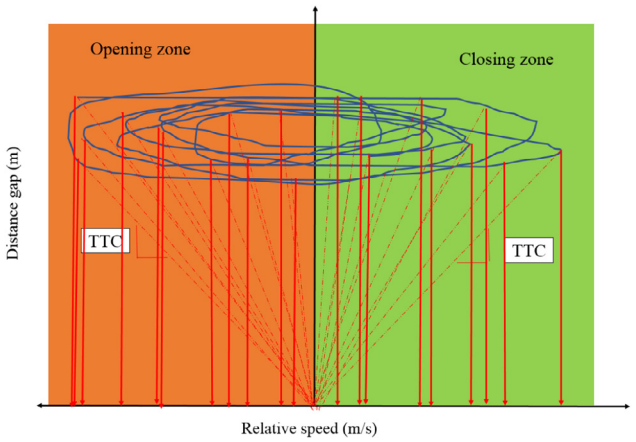


**Fig. 7.** Conceptualized hysteresis plot, explaining TTC computations.

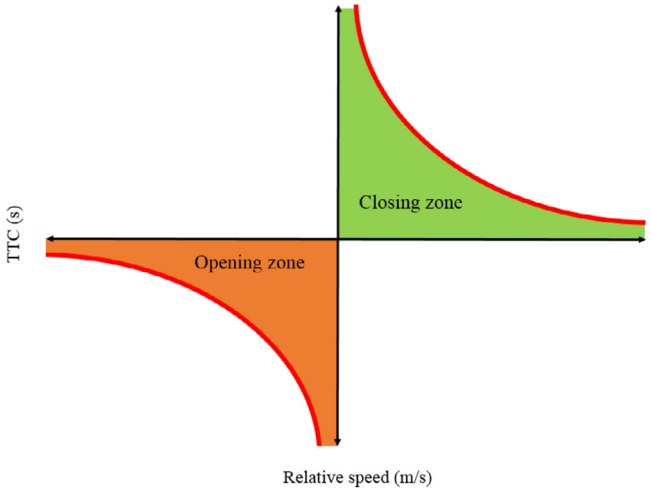


**Fig. 8.** Rectangular hyperbolic formulation depicting opening and closing processes in vehicle-following conditions.

### 4.3. Follower responsiveness

To sense the vehicular interactions, previous studies adopted TTC as a metric to analyze the collision chances. At the same time, certain limitations are associated with TTC. For instance, if the vehicles' relative speed decreases, the TTC value can be nearly infinite. But in a realistic sense, the distance gap between the vehicles plays a critical role in this aspect. In this direction, numerous studies [2,36] supported this inference. Simultaneously, in contrast, the TTC's linearity assumption, the collision risk of the intended way of follower vehicle against the leader vehicle, can be overpredicted given the higher relative speed. To express the linearity assumption an example is presented. For example, for Scenario 1 the follower sensed it leader at $Fv = 20$ m/s, $Lv = 10$ m/s and distance gap $= 20$ m. Thus,

$$\text{TTC} = \frac{distance\,gap}{relative\,speed} = \frac{(20)}{(20-10)} = 2s \tag{11}$$

Scenario 2, the follower sensed it leader at $Fv = 40$ m/s, $Lv = 20$ m/s and distance gap $= 40$ m. Thus,

$$\text{TTC} = \frac{distance\,gap}{relative\,speed} = \frac{(40)}{(40-20)} = 2\,s \tag{12}$$

Further, in both the scenarios, the TTC between the vehicles is the same with 2 s and depicting similar chances for rear-end collisions. Given the perception of follower vehicle, the collision chances in both the scenarios are different in a realistic feel. In scenario 2, the follower has a 40 m distance gap; during the closing phase, the follower vehicle had chance to adjust its movement, and the follower may or may not maintain the same speed.

From the hysteresis and hyperbola pattern analysis, it is implied that determining the follower driver's attention towards its leader driver can be especially useful in quantifying the current safety level in the traffic stream. On these

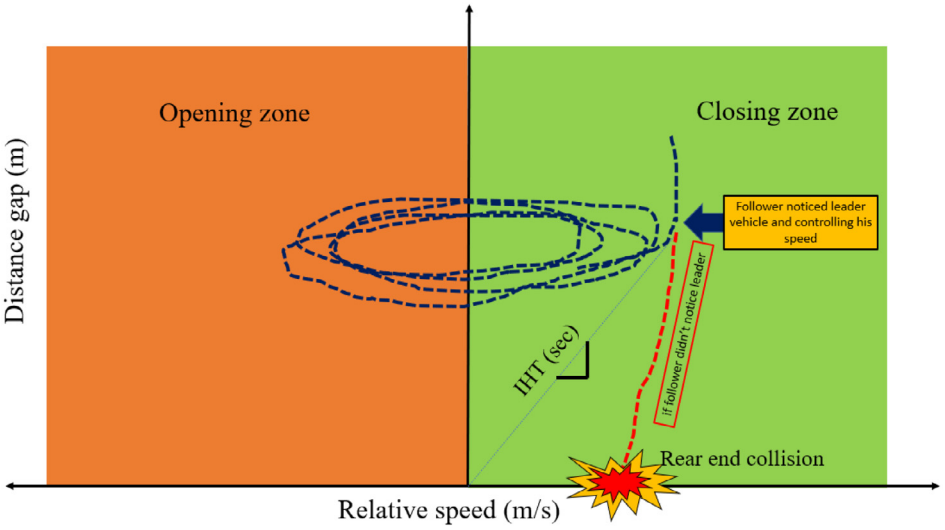


**Fig. 9.** Schematic diagram explaining IHT concept.

lines, when a follower driver approaches its leader, DG is decreased. Over the road space, the follower recognizes that the driver is moving closer to its leader. Hence, to avoid a rear-end collision with the leader, the follower starts to decelerate and tries to match the leader's speed. The phenomenon takes place mainly based on the time available for the follower to decelerate and avoid a rear-end collision. This time is referred to herein as Instantaneous Heeding Time (IHT). To better explain, an example is presented in Fig. 9, where the follower controlled its speed after perceiving the leader's movement, which results in different shapes of the DG vs. RS relation. From Fig. 9, IHT for the subject follower is computed as the slope of the line. Which connects the point with maximum RS on the positive side and the origin. This indicates that the heeding phase is critical in predicting rear-end collisions or near rear-end collisions in the traffic stream.

It can be noted, especially during the heeding phase, that when the follower perceives the leader's movement, the follower decreases speed and tries to match the leader speed to avoid a rear-end collision. For hysteresis at heeding, RS is positive and is likely to experience a local maximum as observed in real-field conditions.

On these lines IHT is given as,

$$IHT(t) = \begin{cases} \frac{X_L(t) - X_F(t) - l}{Fv(t) - Lv(t)} & \forall \begin{bmatrix} Follower\ drops\ its\ speed, Fv\,(t_n) > Fv\,(t_{n+1})\,; \\ \frac{\partial (Fv)}{\partial (t)} = 0; \\ Fv(t) - Lv(t) > 0; \\ \frac{\partial (time\ gap)}{\partial (t)} = 0\ (local\ maxima) \\ time\ gap > 0; \end{bmatrix} \\ \nexists IHT & other\ wise \end{cases} \tag{13}$$

Where
$X_L$ = longitudinal position of the leader vehicle (m)
$X_F$ = longitudinal position of the follower vehicle (m)
$Fv$ = longitudinal speed of the follower vehicle (m/s)
$Lv$ = longitudinal speed of the leader vehicle (m/s)
$l$ = length of the leader vehicle (m)

The IHT value may or may not be the minimum TTC (positive value) between the vehicles, as it depends on the follower and leader positions on given road space and naturally their speeds. Making this as a governing principle an algorithm was developed to compute the IHT using the hysteresis phenomenon derived from trajectory data, as shown in Fig. 10.

Based on the programmed algorithm, IHT is computed for different leader–follower pairs. Further, to explore the nature of its variation, the computed IHT values are correlated with RS and overlaid on the rectangular hyperbola plots, as shown in Fig. 11. It can be observed that the IHT points are scattered over the closing zone in the hyperbola (first quadrant) and corroborate the previous discussion, thereby validating the IHT concept. This shows that the proposed theory holds a good promise for predicting rear-end collisions when the vehicle-following phenomenon occurs in the traffic stream. Under mixed traffic conditions, this can be much more appreciated based on the staggered and overlapped following drivers' behavior. Mixed traffic conditions include different types of vehicles with diverse static and dynamic characteristics. By their sizes and mechanical properties, even driver behavior can be well studied. The IHT concept was explored more comprehensively to predict rear-end collisions in the mixed traffic stream.

Input: Vehicular trajectory data
For (subject vehicle)
  Identify subsequent vehicles and compute lateral overlaps among them
End
For (vehicles with lateral overlap)
  Compute longitudinal distances
  Assemble them as leader-follower pairs
End
For (each pair)
  Compute DG and RS
End
Main loop (all pairs data)
  For (each pair)
    Compute TTC among the pairs
    If (TTC ≥ 0)
      If (Subject follower drops speed && $\frac{\partial(follower\ velocity)}{\partial(time)} \leq 0$)
        If (Relative speed > 0)
          If (Hysteresis shape varied && $\frac{\partial(TTC)}{\partial(time)} == 0$)
            $IHT = TTC$;
          End If
        End If
      End If
    End If
  End For
End Main loop
Output: Finally, IHT is computed for all pairs in the traffic stream

**Fig. 10.** Algorithm scripted in MATLAB for computing IHT.

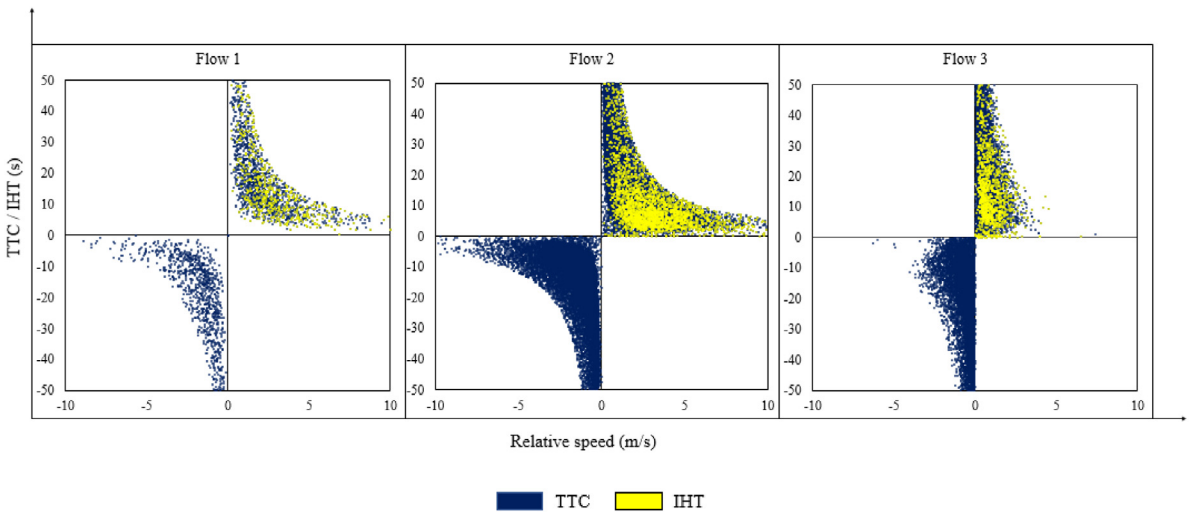


**Fig. 11.** Computed IHT are overlaid on hyperbola plots.

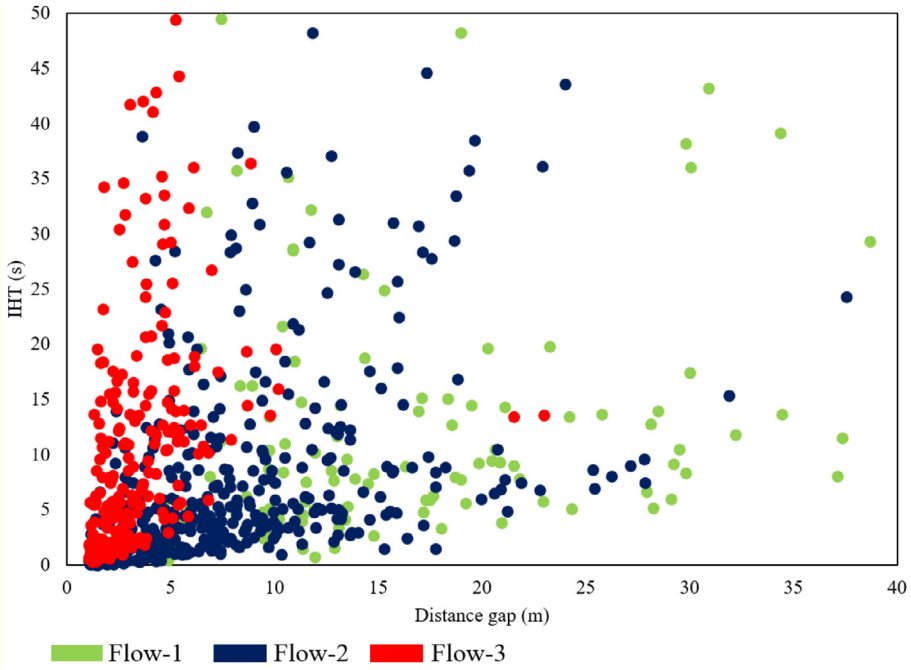


**Fig. 12.** IHT vs distance gap over different flow conditions.

## 5. Safety analysis

### 5.1. Hysteresis analysis

After computing the values of IHT for hysteresis developed using the extracted trajectory data from the mixed traffic streams (Fig. 4), this measure was used to predict the rear-end collisions that result from the following behavior. Based on the analysis, it is realized that pairs with larger IHT values demonstrated the follower's right attentiveness, as it indicates a more significant time gap towards the leader and vice versa. It is also noted that along with IHT, the context at which the follower paid attention towards the leader plays a vital role in a potential rear-end collision. To better understand this, the computed IHT values were also correlated with DG among the leader–follower pairs for three flow levels: free-flow (Flow 1), near-capacity flow (Flow 2), and congested flow (Flow 3), as shown in Fig. 12. Fig. 12 shows that, with an increase in the traffic flow level, DG tends to decrease significantly. As a result, the data points are found to shift towards the IHT-axis with a steeper slope. This implies that a smaller range of DG and smaller IHTs (due to insufficient deceleration time) present a highly unstable region. Hence, it is essential to monitor these parameters. Also, it can be argued that in addition to the time gap, FV and its position are equally important parameters to be included in the approach for predicting rear-end collisions.

Hence, it is inferred that the odds of having a rear-end collision is higher for the pairs with small IHT and small DG, but relatively higher following vehicle speed, and vice-versa. The situations are explained in a self-explanatory qualitative plot, as shown in Fig. 13. As noted, there are broadly three zones of rear-end collisions with different safety levels: high-probability zone, moderated-probability zone, and low-probability zone. The high-probability region implies that with relatively larger FV and insufficient IHT, there is a high probability of a collision. This probability is reduced as IHT and DG increase. Hence, all these factors should be considered comprehensively to predict the possible number of potential rear-end collisions.

As discussed earlier, in addition to available IHT and DG, the follower's speed at which the driver perceived the leader plays a crucial role in predicting a rear-end collision. For example, consider two scenarios. In Scenario 1, the follower moves at 100 km/h and perceives a leader moving at 80 km/h at DG = 20 m. In Scenario 2, the follower moves at 40 km/h and senses a leader moving at 20 km/h with DG = 20 m. It can be observed that in both scenarios, IHT = 1 s and DG = 20 m, tend to display similar chances for rear-end collisions. However, the probability of a rear-end collision for Scenario 1 is expected to be larger than that of Scenario 2. The follower is moving at a more considerable speed when it perceives the leader.

To better understand this phenomenon, the leader–follower pairs developed from the extracted trajectory data were closely examined. Further, the changes in DG, RS, FV, and TTC over time are shown in Fig. 14 for a specific follower pair. For example, in Pair 2, the follower perceived its leader, while the follower is moving at 10 m/s around DG = 25 m, with

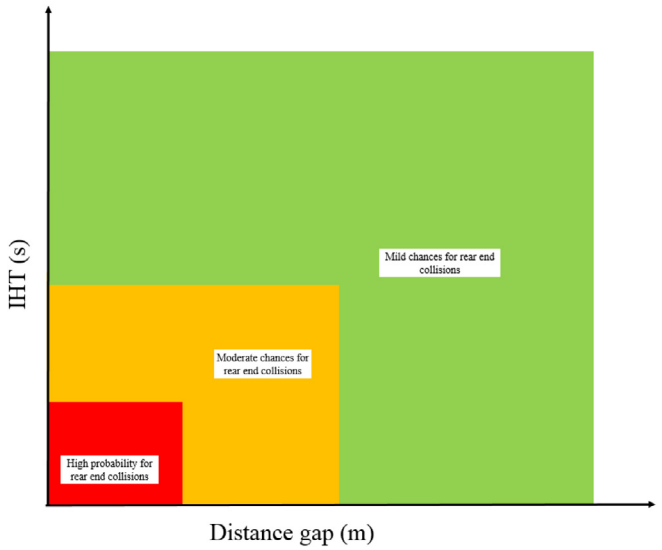


**Fig. 13.** Schematic diagram explaining the importance of IHT and DG for rear end collisions.

IHT = 3.57 s. As noted, IHT is inclusive of RS and can well cater to the logic of rear-end collision. Also, all parameters are significantly independent of each other and dependent on the subject vehicle's behavior. The probability of a rear-end collision depends on three imperatives parameters and forms a strong basis for building a probability-based concept for predicting potential rear-end collision. Sample calculations for other leader–follower pairs are presented in Appendix.

*Probabilistic Analytics*

As discussed earlier, the event of a rear-end collision can be predicted using probability concepts for different critical situations. An attempt is made to explain this approach towards the occurrence of a rear-end collision involving FV, IHT, and DG while following each other. Let P (Fv) be the probability of FV being greater than the critical speed, P (IHT) be the probability of IHT less than the critical time gap, and P (DG) be the probability of DG being less than the critical distance gap. Again $P\left(Fv^{c}\right)$, $P\left(IHT^{c}\right)$, and $P\left(DG^{c}\right)$ are the complimentary probabilities of their respective events. The occurrence of a rear end collision is highly expected when the follower is greater than the critical speed, followed by IHT being less than the critical time and DG being less than the critical distance gap. On these lines, the probability of rear end collision is given as $P\left(Fv \cap IHT \cap DG\right)$, as shown in Fig. 15. Hence, based on the addition probability rule, then

$$P\left(Fv \cup IHT \cup DG\right) = P\left(Fv\right)+P\left(IHT\right)+P\left(DG\right)-P\left(Fv \cap IHT\right)-P\left(Fv \cap DG\right)-P\left(IHT \cap DG\right)+P\left(Fv \cap IHT \cap DG\right) \quad (14)$$

Rearranging the terms, the probability of rear-end collision, $P\left(Fv \cap IHT \cap Rd\right)$, is given by

$$\begin{aligned} P\left(Fv \cap IHT \cap DG\right) &= P\left(Fv\right) + P\left(IHT\right) + P\left(DG\right) - P\left(Fv \cap IHT\right) - P\left(Fv \cap DG\right) \\ &\quad - P\left(IHT \cap DG\right) - P\left(Fv \cup IHT \cup DG\right) \end{aligned} \quad (15)$$

Further, the probability of not having a rear-end collision is given by

$$P\left(Rear\ end\ collsions^{c}\right) = 1 - P\left(Rear\ end\ collisions\right) \quad (16)$$

## 6. Practical implementation

From the available literature, it is noted that there are no such clear findings on applying parameters such as critical speed, IHT, and DG for predicting the probability of occurrence of rear-end collisions. Therefore, in line with Shi et al. [37]'s research work, the parameter thresholds are sensitized. For this purpose, parameter sets with five values are considered: IHT (s) [0.5, 1.5, 2.5, 3.5, 4.5], DG (m) [5, 10, 15, 20], and FV (km/h) [30, 50, 70]. Taking these values as thresholds, safety analysis is performed using a MATLAB code. In the safety analysis, the number of likely rear-end collisions are determined, as shown in Table 4.

Interestingly, for Flow 3, no rear-end collision points are predicted when all thresholds were checked. Compared to Flow 1, for Flow 2, potential rear-end collision points are predicted. This trend is attributed to the variation in all parameters (RS, DG, and IHT) simultaneously. During the steady-state free-flow conditions, DG may be enough for a given value of IHT. However, when a large DG is not available, and RS is considerable, mainly due to the follower's speed, a rear-end collision is possible. When traffic flow transitions from free flow to near-capacity flow, the analysis reveals that

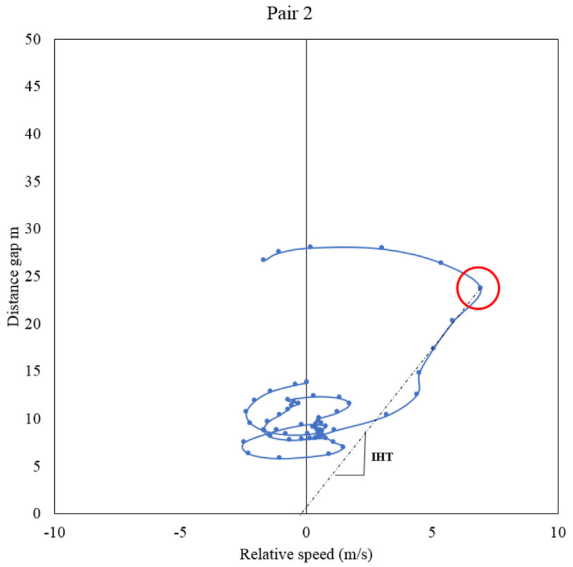


(a) Conceptual explanation of IHT from hysteresis phenomenon

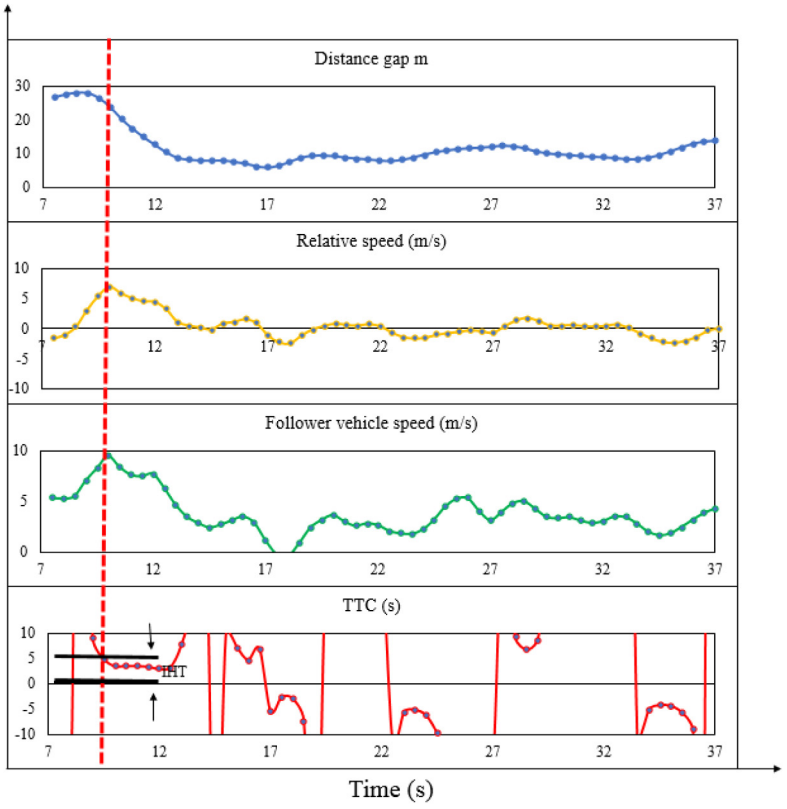


(b) Distance gap, relative speed, follower speed, and TTC over time for the same pair

**Fig. 14.** Hysteresis phenomenon investigated for different set of parameters with time, depicting IHT concept.

there are larger standard deviations in DG, RS, and IHT, which act as major deterrents for the occurrence of rear-end collision.

In Table 5, consider for example a given set of thresholds (IHT = 2.5 s, DG = 10 m, and VS = 30 km/h). For this set, rear-end collisions are analyzed and mapped over the geometry, as depicted in Fig. 16. Concerning the change in flow

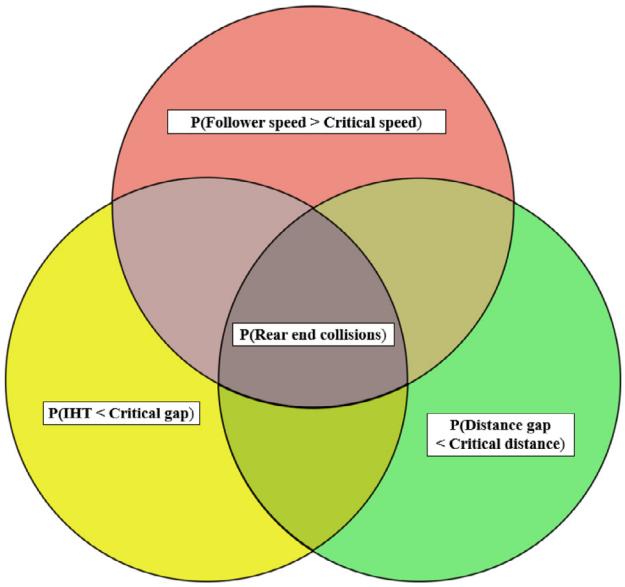


**Fig. 15.** Venn diagram explaining the probability of rear end collisions.

**Table 4**
Count of probable rear-end collision events over various set of thresholds at different traffic flow conditions.

| Follower speed, FV > 30 km/h | | | | | | | | | | | | |
|---|---|---|---|---|---|---|---|---|---|---|---|---|
| DG(m) IHT(s) | Flow 1 | | | | Flow 2 | | | | Flow 3 | | | |
| | <5 | <10 | <15 | <20 | <5 | <10 | <15 | <20 | <5 | <10 | <15 | <20 |
| <0.5 | 3 | 4 | 4 | 4 | 17 | 17 | 17 | 17 | 0 | 0 | 0 | 0 |
| <1.5 | 3 | 4 | 5 | 6 | 32 | 39 | 59 | 62 | 0 | 0 | 0 | 0 |
| <2.5 | 3 | 7 | 9 | 15 | 37 | 41 | 129 | 143 | 0 | 0 | 0 | 0 |
| <3.5 | 3 | 8 | 19 | 34 | 43 | 114 | 216 | 276 | 0 | 0 | 0 | 0 |
| <4.5 | 3 | 10 | 32 | 57 | 44 | 129 | 290 | 405 | 0 | 0 | 0 | 0 |
| Follower speed, FV > 50 km/h | | | | | | | | | | | | |
| <0.5 | 3 | 4 | 4 | 4 | 9 | 9 | 9 | 9 | 0 | 0 | 0 | 0 |
| <1.5 | 3 | 4 | 5 | 6 | 12 | 20 | 26 | 28 | 0 | 0 | 0 | 0 |
| <2.5 | 3 | 6 | 9 | 15 | 12 | 27 | 42 | 48 | 0 | 0 | 0 | 0 |
| <3.5 | 3 | 7 | 18 | 33 | 13 | 28 | 53 | 72 | 0 | 0 | 0 | 0 |
| <4.5 | 3 | 9 | 30 | 55 | 13 | 29 | 65 | 98 | 0 | 0 | 0 | 0 |
| Follower speed, FV > 70 km/h | | | | | | | | | | | | |
| <0.5 | 3 | 4 | 4 | 4 | 0 | 0 | 0 | 0 | 0 | 0 | 0 | 0 |
| <1.5 | 3 | 4 | 5 | 5 | 1 | 3 | 5 | 6 | 0 | 0 | 0 | 0 |
| <2.5 | 3 | 4 | 7 | 10 | 1 | 3 | 6 | 7 | 0 | 0 | 0 | 0 |
| <3.5 | 3 | 4 | 10 | 15 | 1 | 3 | 7 | 11 | 0 | 0 | 0 | 0 |
| <4.5 | 3 | 4 | 12 | 19 | 1 | 3 | 8 | 15 | 0 | 0 | 0 | 0 |

level (mainly Flows 1 and 2), rear-end collision events are predicted as 7 and 41. Based on the analysis, once traffic flow reaches congested flow, traffic safety deterioration appears not to depend on traffic flow. For Flows 1 and 2, a greater number of rear-end collisions are observed, while for Flow 3, data points are clustered on an unlikely zone of rear-end collisions, indicating that their occurrence is almost null. The main reason can be explained as follows. In congested conditions, different vehicle types follow one another, resulting in less RS among vehicle pairs and hence greater IHT values (great attention). This is an indication of uniform traffic flow characteristics in the congestion state. As a result, the data points representing rear-end collisions are grouped in an unlikely zone. Whereas for Flows 1 and 2, there is a wide range of variation in traffic-flow characteristics, wherein sudden changes in RS, IHT, and DG may occur due to randomness and the transition from Flow 1 to Flow 2. To understand the variation in safety for different types of vehicles and involvement of the leader–follower combinations, the same thresholds were used to determine the respective number of rear-end collisions. For this purpose, the same procedure was followed for different vehicle-pairs. The results show that for Flow 1, 25 rear-end collision events are predicted. Interestingly, for Flow 2, the leader of the MTW–MThW pair (smaller aggressive vehicles) tends to show inconsiderate behavior, with 59 probable rear-end collision events compared to other

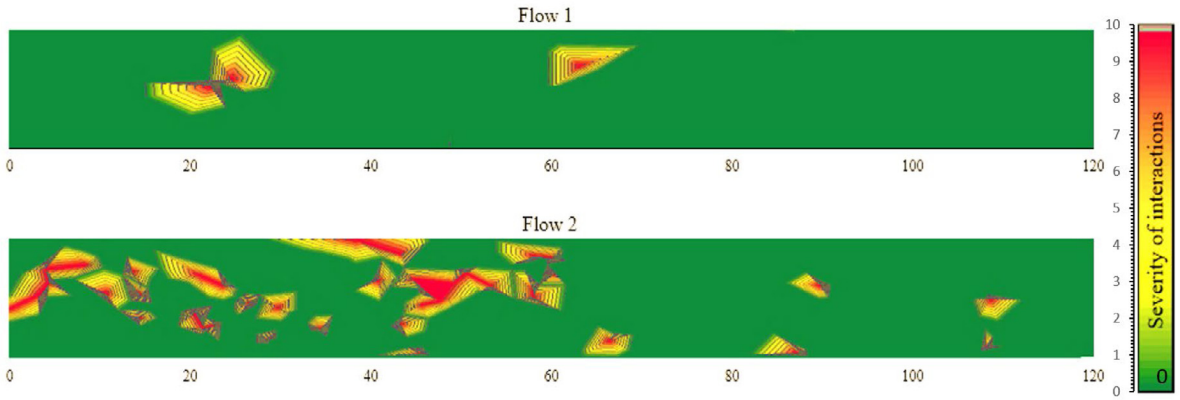


**Fig. 16.** Position of vehicles over the road space, explain the nature of interactions.

**Table 5**
No. of probable rear end collision points over different leader–follower combination.

| | Leader | Follower | | | | | | |
|---|---|---|---|---|---|---|---|---|
| Flow 1_ | | MThW | MTW | Bus | Car | Truck | LCV | Total |
| | MThW | – | – | – | – | – | – | 25 |
| | MTW | 6 | 7 | | 5 | | | |
| | Bus | – | – | – | – | – | – | |
| | Car | – | 4 | – | 2 | – | – | |
| | Truck | – | – | – | – | – | 1 | |
| | LCV | – | – | – | – | – | – | |
| | Leader | Follower | | | | | | |
| | | MThW | MTW | Bus | Car | Truck | LCV | Total |
| Flow 2 | MThW | 9 | 5 | – | 3 | 2 | – | 59 |
| | MTW | 8 | 10 | | 7 | – | | |
| | Bus | – | 4 | – | – | | – | |
| | Car | | 7 | 1 | | 1 | – | |
| | Truck | 2 | – | – | – | – | – | |
| | LCV | – | – | – | – | – | – | |

vehicle categories. Again, the MTW as a follower tended to be aggressive and resulted in a higher number of rear-end collisions.

On the other hand, for Flow 3, with limited lateral freedom to maneuver, vehicles were following one another with larger IHT and lesser RS. As a result, no rear-end collision event is predicted for that traffic level. Hence, it may be inferred that a maximum probability of rear-end collision can exist for Flow 2 (near capacity). For Flow 2 (near capacity), mainly MTW and MThW, tend to have higher lateral freedom due to their size, resulting in aggressiveness to their leaders. Further, these smaller vehicles tend to have inconsiderate behavior towards their followers. Hence, the MTW–MTW, MTW–MThW, MThW–MTW, and MTW–cars are the most vulnerable when following each other under Flow 2 conditions. Also, the pairs of cars–MTW and MThW–Cars are predicted as sensitive pairs for probable rear-end collision events.

Nonetheless, the vehicle pairs involving heavy vehicles are found to be mostly not vulnerable to rear-end collisions on urban arterials. The situation may be different on intercity roads, as drivers can be substantially different in rural environments. This finding is only applicable for urban multilane arterials.

## 7. Summary and conclusions

From the analysis of vehicle-following behavior, it was observed that the leader–follower pairs tend to display the hysteresis phenomenon by fluctuating DG and RS during the following process. Further, concerning the change in traffic flow level, the following behavior involving different vehicle pairs was significantly different. For example, for Flow 1, partial hysteresis loops are observed, whereas, for Flow 2, whole hysteresis loops are found. Moreover, for Flow 3, the hysteresis loops are in slenderer nature, indicating that the follower maintains lesser DG and RS towards the leader.

Further, the study reveals a unique rectangular hyperbolic relationship between TTC and DG, where the hyperbolic form varies with DG. Based on the investigation of rectangular hyperbola analytics, it was observed that DG dictates the hyperbola. For the traffic flow levels, it was observed that for Flow 1, the hyperbola shape was partially visualized due to the lesser following interaction among the pairs. Whereas for Flow 2, a definite full rectangular hyperbola shape was

observed. For Flow 3, in the rectangular hyperbola plots, the data points are clustered towards the TTC axis, indicating a reduction in RS among the pairs in congested traffic flow conditions.

Based on the analysis of the hysteresis and hyperbolic patterns, it was determined that the follower's attention towards its leader plays a significant role in understanding traffic safety over the road sections, mainly predicting rear-end collision. Thus, in the present research, the responsiveness of the follower is captured using hysteresis plots. It was identified that, at the time of the following maneuver, perceiving the leader, the follower will move at a more considerable speed compared with that of the leader. Precisely at the instance of perception, the follower drops the speed based on traffic conditions, RS and TTC will be positive, where further TTC changes the nature at that instant. Typically, TTC quantifies the time gap available for in avoiding a collision at following conditions. Given the mathematical formulation of TTC, the TTC will account higher number of conflicts and can wrongly depict the case. On the other hand, the conceptualized IHT defines the aggressiveness of the follower vehicle towards its leader and represents the action points in following hysteresis phenomena. Like its counterpart TTC, higher IHT depicts less aggression and vice versa. The distance gap DS between the vehicles depicts the decisiveness of the follower vehicle. However, considering IHT and DS will omit the state of the subject vehicle, in which he/she has maintained the IHT and DS. Considering this, the vehicle's speed is included in the safety framework. Thus, IHT is recommended to quantify the follower's attentiveness and hence predict the rear-end collision during the following maneuvers of different vehicle pairs. The insight behind identifying most vulnerable vehicle pairs involving small vehicles (as followers/leaders) is suggested using probability concepts.

Further, the context that the follower response to its leader plays a critical factor in identifying a potential rear-end collision was investigated for different traffic flow levels, leader–follower pairs, and vehicle types. Based on the analysis, it was found that along with IHT, the distance gap and FV are critical factors in identifying potential rear-end collisions. Interestingly, using these parameters, the classical probability-based concept is suggested for evaluating safety over the traffic stream.

With limited studies available in the literature, the critical thresholds for the parameters for predicting rear-end collisions were identified in this study, and safety analysis was performed to understand better the intricacies involved in rear-end collisions. Based on the analysis for different traffic flow levels, it was observed that, when compared to free-flow and near-capacity conditions, a higher number of rear-end collision points are predicted in the traffic stream over the road space, particularly at Flow 2. On the other hand, for congested flow, with limited freedom to move over the road space, the follower is attentive towards the leader with less speed and RS. As a result, no potential rear-end collisions are observed in this case. From this discussion, it has emerged that during the transition from the free flow and near-capacity traffic flow conditions, the valid parameters such as IHT, RS, and DG should be checked simultaneously, suggesting critical thresholds for different vehicle pairs more aptly. Based on this study, the following conclusions are made:

1. Quantifying driving behavior over a given road section is a major factor in understanding the critical elements involved at the micro-level that affect traffic safety. In fulfilling this objective, many researchers reported different TTC measures, particularly for predicting rear-end collisions during vehicle-following behavior. A new safety measure, IHT, was suggested in the present study. Based on investigating TTC and RS's relationship, the study also uncovered the rectangular hyperbolic pattern of driver behavior during vehicle-following situations.
2. Most researchers have focused on the time gap measure for safety assessment. In this study, a suitable methodology for quantifying driver attention under vehicle-following conditions is proposed. The study also uncovered the variation in driving behavior under mixed traffic conditions and explored the smaller vehicles' inconsiderate behavior in the traffic stream.
3. In the coming days, with necessary studies, the critical thresholds for speed, DG, and IHT, the potential rear-end collisions can be quantified better. Further, the methodology can be deployed on a real-time basis in guiding drivers by informing them through in-vehicle notification of the critical parameters to avoid the rear-end collisions. The traffic stream's performance can be improved by enforcing a better level of driver compliance, where rash drivers are penalized with enough evidence.
4. The results show that smaller vehicles(MTWs) in the traffic stream contribute to major share of conflicts, either as a leader or follower. This can be viewed as their propensity for lateral movement in escaping the delay. From the analysis it clearly visible that MTW frequently overtake nearby vehicles and perform many lateral movements in a single lane. This indicates that MTW drivers tend to accept small gaps due to their ease in maneuverability. Thus, MTWs are exposed to lesser IHTs with less DS at high speeds. As a result, the safety level will potentially deteriorate in actual traffic conditions. On similar lines, to improve the traffic safety in the traffic flows with different vehicle combinations, the IHT safety framework, can be help draft policies to enhance safety in the traffic stream, reducing rear-end collisions. Further in recent times, dedicated MTW lanes is viewed as a problem solver for non-lane based mixed traffic. Given this, with IHT the safety impacts in can be studied in best possible manner in quantifying the benefits of dedicated lanes.

## 8. Limitations and future scope

Along with the research findings, the present study has certain limitations, which should be considered in the work's future scope.

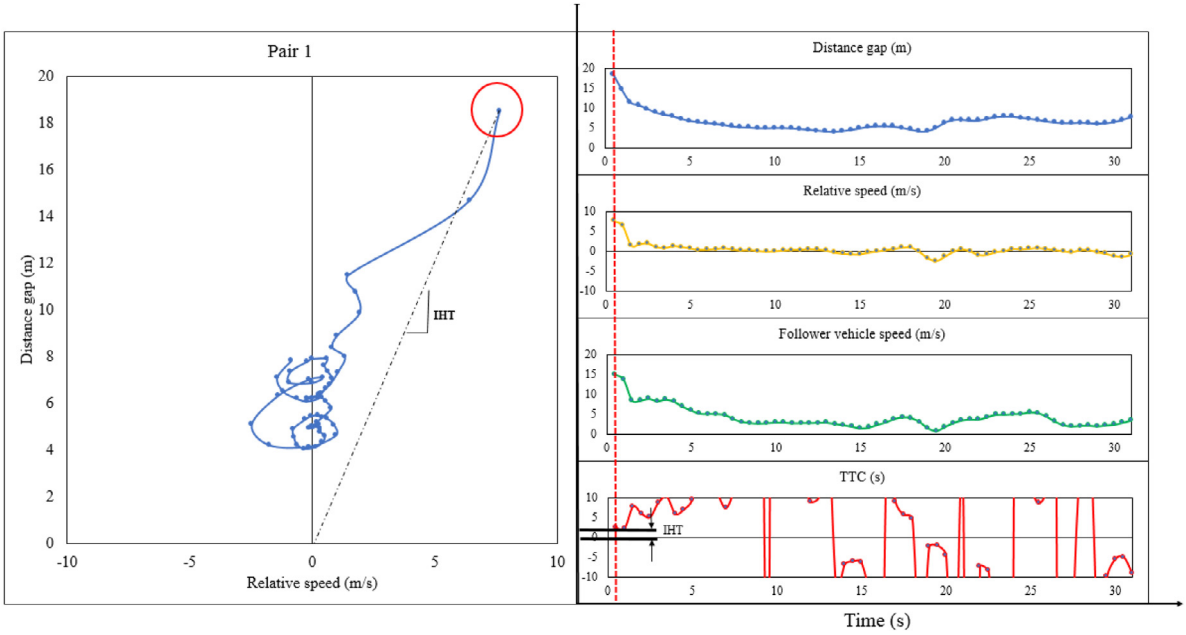


**Fig. 17.** Hysteresis phenomenon investigated over different set of parameters with time, depicting IHT concept.

- The developed IHT and safety framework is tested only on a single study section, with three flow conditions. However, to understand the core formulation stability and the effectiveness in usage, the IHT and safety framework should be tested at different study sections over different flow conditions.
- At the same time, unlike any other surrogate safety measures, in the present study the thresholds are assumed from the literature. Further there is a need for enough studies to establish the thresholds for a better safety analysis.
- In recent times, researchers highlight that a given subject follower vehicle can have multiple leader vehicles in non-lane-based traffic conditions. Considering this, the present IHT can be upgraded for the safety analysis in multiple leader combinations.

## CRediT authorship contribution statement

**Narayana Raju:** Conceptualization, Methodology, Data curation, Writing – original draft, Investigation. **Shriniwas Arkatkar:** Supervision, Investigation, Writing – review & editing. **Constantinos Antoniou:** Supervision, Investigation, Writing – review & editing.

## Declaration of competing interest

The authors declare that they have no known competing financial interests or personal relationships that could have appeared to influence the work reported in this paper.

## Data availability

Data will be made available on request.

## Appendix. Annexure

In section, on an example basis, four leader–follower combinations are presented. On these lines hysteresis plots, followed by DG, RS, FV and TTC are plotted over time as reported in the Figs. 17 to 20. It can be noted in all pairs at that the when the follower perceived the leader, immediately, it stated reducing its speed, RS will be >0, TTC >0 and shift in hysteresis $\frac{\partial(TTC)}{\partial(Time)} = 0$, $\frac{\partial(follower\ velocity)}{\partial(Time)} \leq 0$

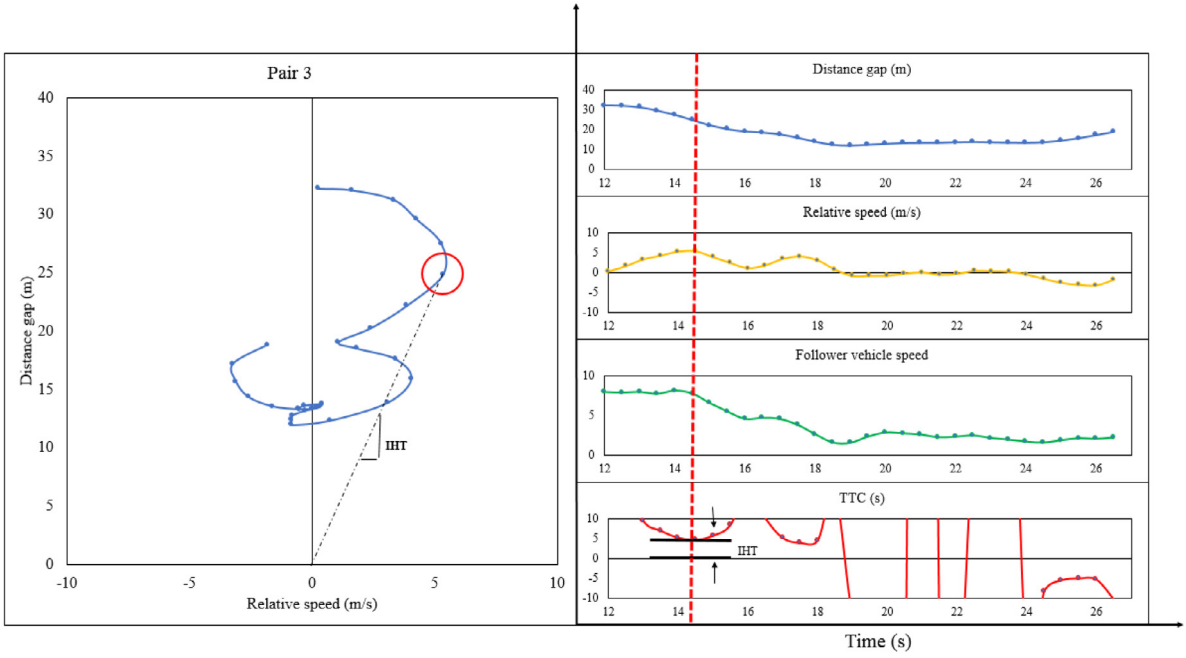


**Fig. 18.** Hysteresis phenomenon investigated over different set of parameters with time, depicting IHT concept.

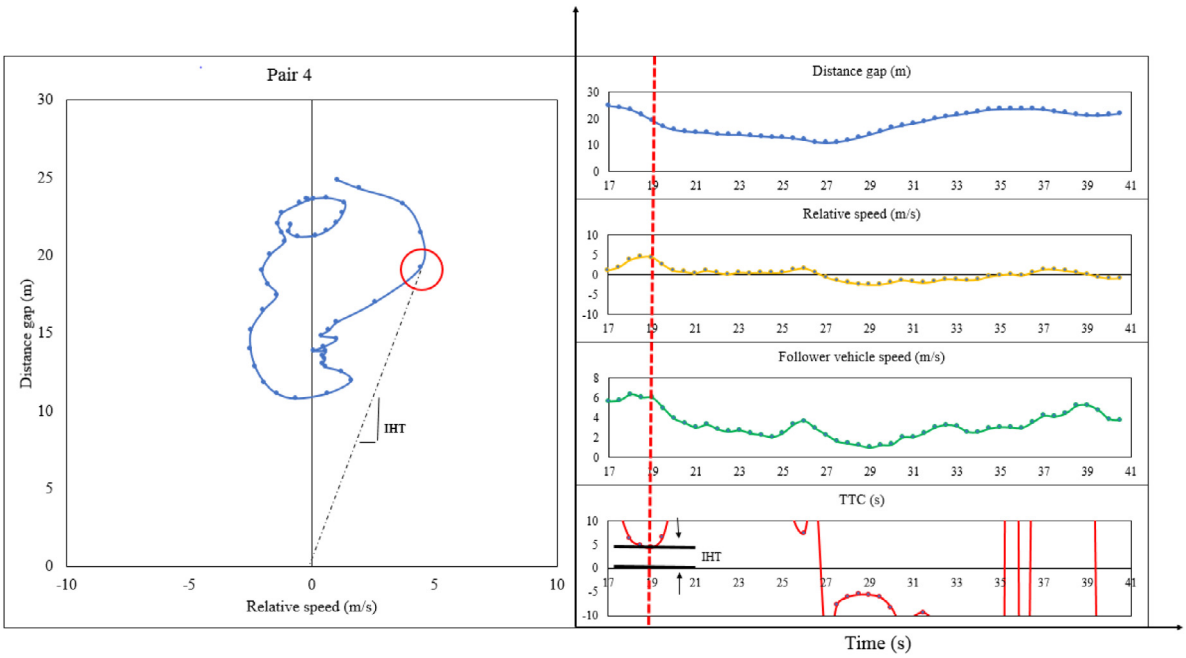


**Fig. 19.** Hysteresis phenomenon investigated over different set of parameters with time, depicting IHT concept.

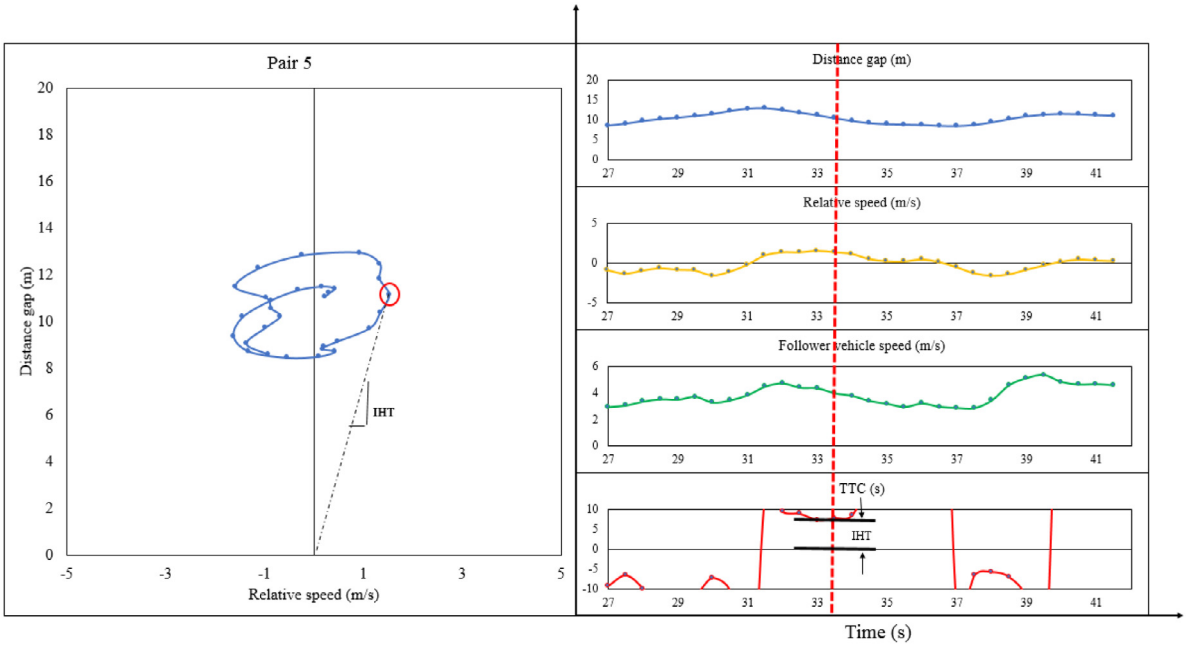


**Fig. 20.** Hysteresis phenomenon investigated over different set of parameters with time, depicting IHT concept.

## References


[1] J.C. Hayward, Near miss determination through use of a scale of danger, Highw. Res. Board 384 (1972).
[2] M.M. Minderhoud, P.H.L. Bovy, Extended time-to-collision measures for road traffic safety assessment, Accid. Anal. Prev. (2001) http://dx.doi.org/10.1016/S0001-4575(00)00019-1.
[3] Q. Meng, X. Qu, Estimation of rear-end vehicle crash frequencies in urban road tunnels, Accid. Anal. Prev. (2012) http://dx.doi.org/10.1016/j.aap.2012.01.025.
[4] S. Almqvist, C. Hyden, R. Risser, Use of speed limiters in cars for increased safety and a better environment, Transp. Res. Rec. (1991).
[5] F. Cunto, F.F. Saccomanno, Calibration and validation of simulated vehicle safety performance at signalized intersections, Accid. Anal. Prev. (2008) http://dx.doi.org/10.1016/j.aap.2008.01.003.
[6] C. Johnsson, A. Laureshyn, T. De Ceunynck, In search of surrogate safety indicators for vulnerable road users: A review of surrogate safety indicators, Transp. Rev. 38 (6) (2018) http://dx.doi.org/10.1080/01441647.2018.1442888.
[7] R. Van Der Horst, J. Hogema, Time-to-collision and collision avoidance systems, in: Proceedings of the 6th Workshop of the International, 1993, doi:10.1.1.511.3548.
[8] C. Schwarz, On computing time-to-collision for automation scenarios, Transp. Res. F (2014) http://dx.doi.org/10.1016/j.trf.2014.06.015.
[9] R.S. Jurecki, T.L. Stańczyk, Driver reaction time to lateral entering pedestrian in a simulated crash traffic situation, Transp. Res. F (2014) http://dx.doi.org/10.1016/j.trf.2014.08.006.
[10] C. Oh, T. Kim, Estimation of rear-end crash potential using vehicle trajectory data, Accid. Anal. Prev. 42 (6) (2010) 1888–1893, http://dx.doi.org/10.1016/j.aap.2010.05.009.
[11] J. Appiah, F.A. King, M.D. Fontaine, B.H. Cottrell, Left turn crash risk analysis: Development of a microsimulation modeling approach, Accid. Anal. Prev. (144) (2020) http://dx.doi.org/10.1016/j.aap.2020.105591.
[12] O. Giuffrè, A. Granà, M.L. Tumminello, T. Giuffrè, S. Trubia, A. Sferlazza, M. Rencelj, Evaluation of roundabout safety performance through surrogate safety measures from microsimulation, J. Adv. Transp. 2018 (2018) http://dx.doi.org/10.1155/2018/4915970.
[13] Y. Guo, T. Sayed, L. Zheng, M. Essa, An extreme value theory based approach for calibration of microsimulation models for safety analysis, Simul. Model. Pract. Theory (106) (2021) http://dx.doi.org/10.1016/j.simpat.2020.102172.
[14] B. Lv, R. Sun, H. Zhang, H. Xu, R. Yue, Automatic vehicle-pedestrian conflict identification with trajectories of road users extracted from roadside LiDAR sensors using a rule-based method, IEEE Access 7 (2019) http://dx.doi.org/10.1109/ACCESS.2019.2951763.
[15] J. Stipancic, S. Zangenehpour, L. Miranda-Moreno, N. Saunier, M.A. Granié, Investigating the gender differences on bicycle-vehicle conflicts at urban intersections using an ordered logit methodology, Accid. Anal. Prev. 97 (2016) http://dx.doi.org/10.1016/j.aap.2016.07.033.
[16] L. Zheng, C. Zhu, Z. He, T. He, S. Liu, Empirical validation of vehicle type-dependent car-following heterogeneity from micro- and macro-viewpoints, Transportmetrica B 7 (1) (2019) http://dx.doi.org/10.1080/21680566.2018.1517057.
[17] E. Ka, D.G. Kim, J. Hong, C. Lee, Implementing surrogate safety measures in driving simulator and evaluating the safety effects of simulator-based training on risky driving behaviors, J. Adv. Transp. 2020 (2020) http://dx.doi.org/10.1155/2020/7525721.
[18] F. Orsini, G. Gecchele, M. Gastaldi, R. Rossi, Collision prediction in roundabouts: A comparative study of extreme value theory approaches, Transportmetrica A 15 (2) (2019) http://dx.doi.org/10.1080/23249935.2018.1515271.
[19] X. Yan, M. Abdel-Aty, E. Radwan, X. Wang, P. Chilakapati, Validating a driving simulator using surrogate safety measures, Accid. Anal. Prev. (2008) http://dx.doi.org/10.1016/j.aap.2007.06.007.
[20] A. Calvi, F. D'Amico, C. Ferrante, L. Bianchini Ciampoli, Effectiveness of augmented reality warnings on driving behaviour whilst approaching pedestrian crossings: A driving simulator study, Accid. Anal. Prev. (147) (2020) http://dx.doi.org/10.1016/j.aap.2020.105760.
[21] A. Sobhani, B. Farooq, Impact of smartphone distraction on pedestrians' crossing behaviour: An application of head-mounted immersive virtual reality, Transp. Res. F 58 (2018) http://dx.doi.org/10.1016/j.trf.2018.06.020.

[22] Z. Xu, X. Zou, T. Oh, H.L. Vu, Studying freeway merging conflicts using virtual reality technology, J. Saf. Res. 76 (2021) http://dx.doi.org/10.1016/j.jsr.2020.11.002.
[23] W. Chen, Y. Liu, Gap-based automated vehicular speed guidance towards eco-driving at an unsignalized intersection, Transportmetrica B 7 (1) (2019) http://dx.doi.org/10.1080/21680566.2017.1365661.
[24] N. Raju, S. Arkatkar, S. Easa, G. Joshi, Customizing the following behavior models to mimic the weak lane based mixed traffic conditions, Transportmetrica B (2021) http://dx.doi.org/10.1080/21680566.2021.1954562.
[25] D. Stavrinos, J.L. Jones, A.A. Garner, R. Griffin, C.A. Franklin, D. Ball, S.C. Welburn, K.K. Ball, V.P. Sisiopiku, P.R. Fine, Impact of distracted driving on safety and traffic flow, Accid. Anal. Prev. (2013) http://dx.doi.org/10.1016/j.aap.2013.02.003.
[26] X. Yan, M. Abdel-Aty, E. Radwan, X. Wang, P. Chilakapati, Validating a driving simulator using surrogate safety measures, Accid. Anal. Prev. 40 (1) (2008) 274–288, http://dx.doi.org/10.1016/j.aap.2007.06.007.
[27] G. Asaithambi, V. Kanagaraj, K.K. Srinivasan, R. Sivanandan, Study of traffic flow characteristics using different vehicle-following models under mixed traffic conditions, Transp. Lett. 10 (2) (2018) 92–103, http://dx.doi.org/10.1080/19427867.2016.1190887.
[28] G. Lanzaro, T. Sayed, R. Alsaleh, Can motorcyclist behavior in traffic conflicts be modeled? A deep reinforcement learning approach for motorcycle-pedestrian interactions, Transportmetrica B (2021) http://dx.doi.org/10.1080/21680566.2021.2004954.
[29] N. Raju, P. Kumar, A. Jain, S.S. Arkatkar, G. Joshi, Application of trajectory data for investigating vehicle behavior in mixed traffic environment, Transp. Res. Rec.: J. Transp. Res. Board 97 (2018) http://dx.doi.org/10.1177/0361198118787364.
[30] N. Raju, S. Arkatkar, G. Joshi, Study of vehicle following behaviour under heterogenous traffic conditions, in: Traffic Granular Flow 2017, Springer International Publishing., 2019, pp. 87–95, http://dx.doi.org/10.1007/978-3-030-11440-4_11.
[31] P. Kumar, N. Raju, A. Mishra, S.S. Arkatkar, G. Joshi, Validating area occupancy-based passenger car units and homogeneous equivalent concept under mixed traffic conditions in India, J. Transp. Eng. A (2018) http://dx.doi.org/10.1061/JTEPBS.0000184.
[32] H. Azami, K. Mohammadi, B. Bozorgtabar, An improved signal segmentation using moving average and Savitzky-Golay filter, J. Signal Inform. Process. (2012) http://dx.doi.org/10.4236/jsip.2012.31006.
[33] N. Raju, P. Kumar, C. Reddy, S. Arkatkar, G. Joshi, Examining smoothening techniques for developing vehicular trajectory data under heterogeneous conditions, J. East. Asia Soc. Transp. Stud. 12 (2017) 1549–1568.
[34] R. Wiedemann, Simulation Des Strazenverkehrsflusses, 1974th ed., Univ. Inst. für Verkehrswesen, Karlsruhe, 1974, 1974.
[35] D.N. Lee, A theory of visual control of braking based on information about time to collision, 1976, Perception.
[36] C. Laugier, I.E. Paromtchik, M. Perrollaz, M. Yong, J.D. Yoder, C. Tay, K. Mekhnacha, A. Nègre, Probabilistic analysis of dynamic scenes and collision risks assessment to improve driving safety, IEEE Intell. Transp. Syst. Mag. (2011) http://dx.doi.org/10.1109/MITS.2011.942779.
[37] L. Shi, Y. Han, H. Huang, Q. Li, B. Wang, K. Mizuno, Analysis of pedestrian-to-ground impact injury risk in vehicle-to-pedestrian collisions based on rotation angles, J. Saf. Res. 64 (2018) 37–47.